Data-Replay Analysis of LAAS Safety during Ionosphere Storms

Young Shin Park, Godwin Zhang, Sam Pullen, Jiyun Lee, and Per Enge
Stanford University

ABSTRACT

As reported in [2,4,5], previous Stanford research has identified the potential for severe ionosphere spatial gradients to affect Local Area Augmentation System (LAAS) integrity. In previous work [1], real-time position-domain geometry screening was used to maximize LAAS availability in the presence of ionosphere anomalies by broadcasting an inflated value of σ_{vig} so that the maximum-ionosphere-induced-error-in-vertical (MIEV) for all viable airborne "subset" geometries (subsets of the set of satellites visible to and approved by the LGF) is below a pre-determined safe limit. The results of this work are based on the LAAS ionosphere spatial-gradient "threat model" established and validated with ionosphere storm data observed from WAAS and IGS since 2000 [2,4]. This previous approach leads to marginal availability of the required integrity (95 to 99 percent) and does not give the higher availability that is desired (99.9 percent or higher).

In this paper, data from the Ohio cluster of CORS stations on November 20, 2003 and the North Carolina cluster of CORS stations on October 29, 2003 from [6] are used to perform "data-replay" analysis for several independent station pairs with separations from 23 to 75 km. These separations are significantly further than the effective LAAS user-to-LGF separation at the CAT I decision height. Comparisons of the result of data-replay analysis with the result of worst-case simulation in the manner of [1] are made. The conclusion derived from these comparisons is that CAT I ionosphere analysis performed by worst-case simulation is conservative but not unreasonable.

1.0 INTRODUCTION

The Local Area Augmentation System (LAAS) was designed to insure the integrity of broadcast pseudorange corrections by monitoring of measured satellite pseudo-ranges within the LAAS Ground Facility (LGF). This monitoring allows the LGF to ensure that errors in the LGF pseudorange corrections are bounded (to the required integrity probability) by the nominal error sigmas that are broadcast with them (within the LGF, measurements that fail one or more monitors are excluded so that they cannot be applied by LAAS users). This procedure allows aircraft receiving LAAS corrections to compute "protection levels" and thus determine the integrity of any set of satellites visible at the aircraft as long as each satellite has a pseudorange correction, sigma values, and "B-values" broadcast for it [1].

One of the residual errors that can build up for the user of a differential GPS system like LAAS is ionosphere spatial decorrelation error. This error is caused by the fact that two GPS signals are passing through different regions of the atmosphere, and the resulting ionosphere delays cannot be completely canceled out even after applying differential corrections. Under severe ionosphere storm conditions, these errors can grow large enough to pose a threat to user integrity.

Several ionosphere storms of concern have occurred since the April 2000 storm that first alerted us to this potential hazard. Among them, the two largest ones were on October 29-30, 2003 and November 20, 2003. Figure 1 shows a snapshot of the ionosphere delay map over CONUS on October 29, 2003 between 20:00 to 20:45 UT. The *x*-axis and *y*-axis represent longitude and latitude, respectively. The color scale indicates the magnitude of the vertical ionosphere delay [2]. Dark red represents about 20 meters of delay, and dark blue represents about 2 meters. As can be seen, there are some sharp transitions between the dark red and the blue, which indicates sharp spatial gradients in those areas. By comparing the subplots, it appears that the storm did not move much (relative to the continental scale shown) during the 45 minutes covered by the subplots. An ionosphere movie made to show that period with finer time resolution also indicates that the anomaly may have been "near stationary" at specific locations and times.

Figure 2 shows the November 20, 2003 storm in a similar fashion. This time, only the eastern half of the U.S. is shown. The large anomaly feature appears different than

what was seen previously (i.e., it has a distinctive "finger shape" in it), and it appears to move faster in general. However, additional sharp gradients between dark red and blue zone are observed [2].

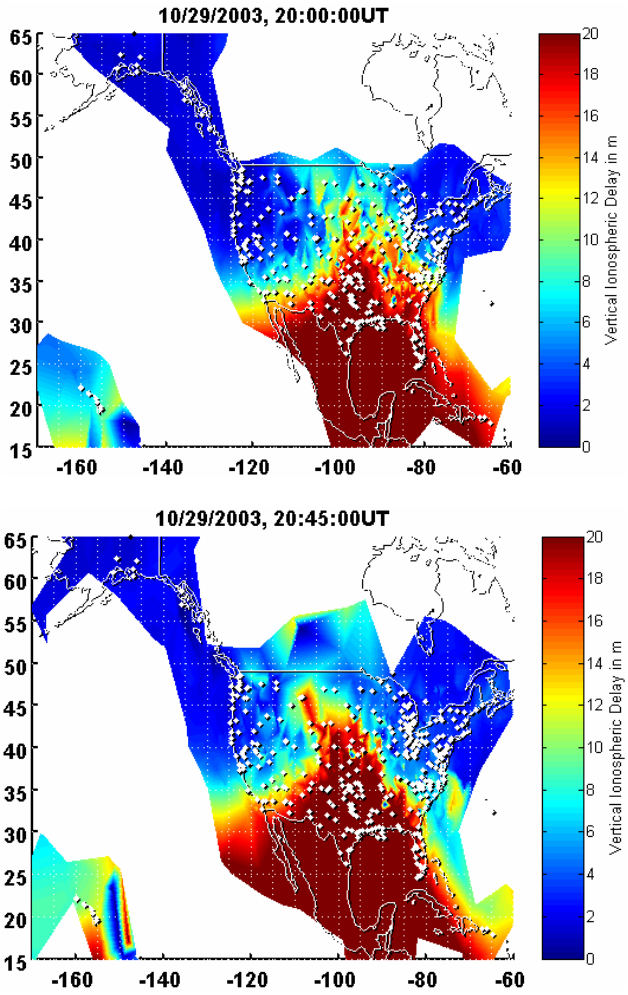

Figure 1: Ionosphere Spatial Anomalies Observed during October 29, 2003 Storm

As described in our previous work (see [5,9,10]), ionosphere anomalies are modeled as linear wave fronts in order to study their impact on a LAAS user. Figure 3 illustrates this simplified model. The gradient represents a linear change in vertical ionosphere delay between the "high" and "low" delay zones. Four parameters are used to characterize the anomaly: gradient slope (in mm/km), gradient width (in km), front speed (in m/s), and maximum delay difference (in m), which is simply the product of gradient slope and width. Upper bounds on each of these parameters have been determined based on analysis of past storms, including the October 29-30 and November 20, 2003 storms. Note that the maximum delay difference is also expressed as an upper bound in this model, and it constrains the slope and width values through their product (i.e., values of slope and width which are within their respective bounds but exceed the maximum-delay-difference bound when multiplied together are not a valid combination) [2,4].

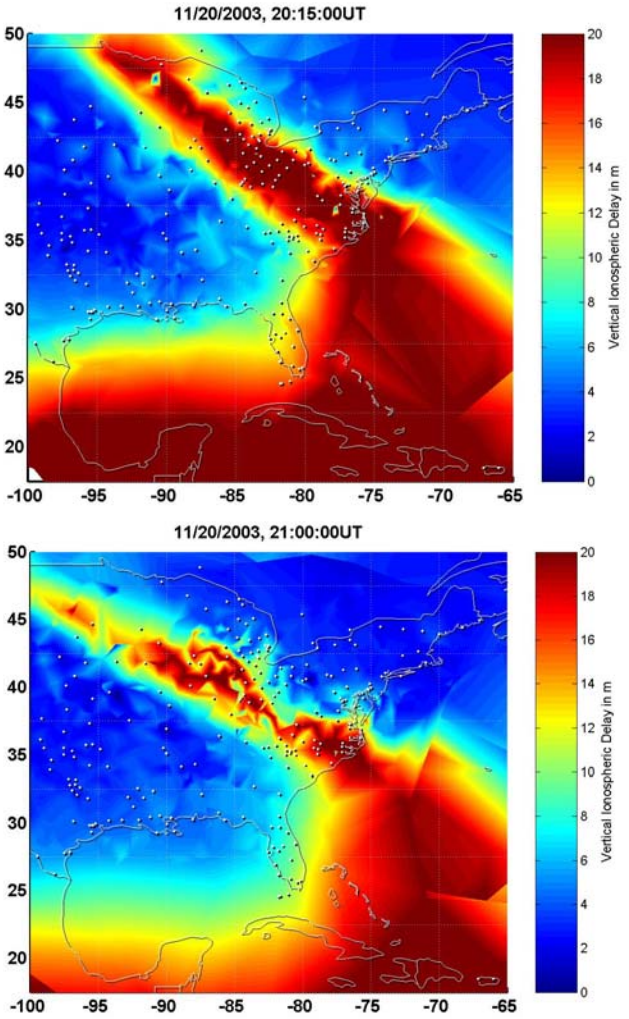

Figure 2: Ionosphere Spatial Anomalies Observed during November 20, 2003 Storm

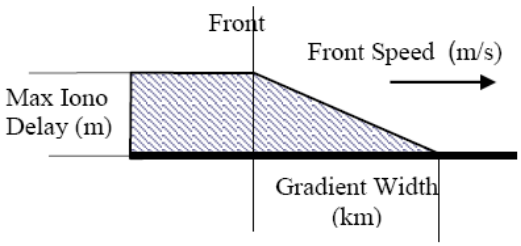

Figure 3: Simplified Model of Ionosphere Anomaly

While almost all anomalies that pose a threat to LAAS can be mitigated completely within the range domain, severe ionosphere spatial anomalies must be handled differently. Very large ionosphere spatial gradients

observed in CONUS during ionosphere storms in October and November 2003 could have created range-domain errors of several meters before being detected by LGF monitoring [2,5]. The magnitude of these potential errors exceeds what can be bounded in the range domain. In other words, aircraft satellite geometries that appear usable due to the vertical protection level (or VPL) being below the specified "safe" vertical alert limit (or VAL) for CAT I precision approaches (VAL = 10 meters at the minimum CAT I decision height of 200 ft) are safe with respect to nominal conditions and almost all failure modes but may not be safe in the presence of a worst-case ionosphere anomaly. Therefore, satellite geometry screening, or position-domain verification that each geometry potentially usable at the aircraft is safe in the presence of the worst-case ionosphere-anomaly threat, is required. Our previous paper demonstrates that position-domain geometry screening in LAAS can fully mitigate the CONUS ionosphere spatial decorrelation threat model [1]. A summary of this screening procedure is shown on the left-hand side of Figure 5.

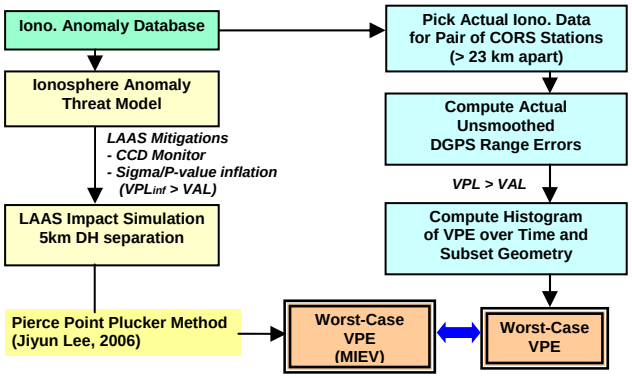

Figure 5: Simulation versus Data-Replay Analysis

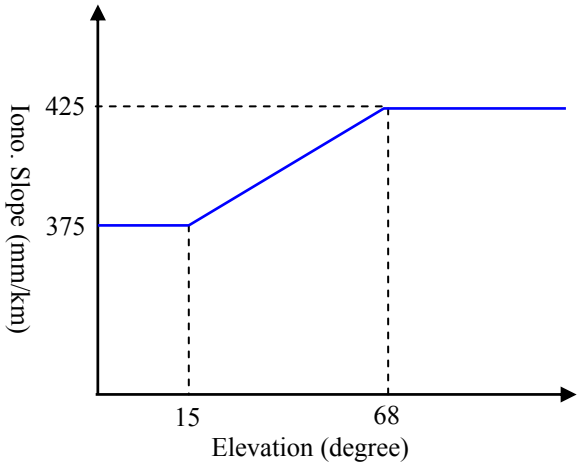

Figure 6: Ionosphere Anomaly Threat Model (Slope Bounds Last Updated in March 2007)

As noted above, the parameters in the simplified model of ionosphere anomaly are estimated using data collected on ionosphere stormy days, and they can be summarized by an ionosphere anomaly "threat model". The current threat model (most recently revised in March 2007) is as shown in Figure 6, in which the ionosphere slope is 375 mm/km for low satellite elevation and 425 mm/km for high satellite elevation (the bounds on speed, width, and maximum delay difference remain the same as the numbers given in [1]). Next, LAAS mitigations such as the LGF code-carrier divergence (CCD) monitor, which detects high ionosphere rates-of-change that are observable to the LGF, and any sigma/P-value inflation implemented for geometry screening are applied. Then, LAAS impact simulations are performed to get the worst-case vertical protection error (VPE), which is commonly known as the maximum ionosphere error in vertical position (or MIEV) are conducted. The "Pierce Point Plucking" or "PPP" method described in [1], which is the current method used in ionosphere mitigation simulation, considers worst-case ionosphere impacts on all possible pairs of satellites and is thus seen to be conservative.

As originally conceived in previous work (see [2,3]), a process known as "data-replay analysis" has been developed to demonstrate that the results obtained by simulation (based on the conservative approach described above) can reasonably approximate the result that is achieved by using observed anomalous data between two fixed WAAS or CORS reference-station locations that were also used to estimate the parameters of the ionosphere threat model. Therefore, actual ionosphere data from the same ionosphere anomaly database was picked for pairs of CORS stations to compute unsmoothed DGPS Range Errors. Applying "baseline" geometry screening (meaning that sigmas are not inflated to further constrain user geometries), VPE for each usable subset geometry and histograms of VPE over subset geometry and time were obtained. Finally, the worst-case VPE (or MIEV) is obtained and is compared to the worst-case VPE obtained by simulation.

2.0 DATA AND ANALYSIS PROCEDURE

2.1 Data

In this paper, data from the Ohio (OH) cluster of CORS stations on November 20, 2003 and from the North Carolina (NC) cluster of CORS stations on October 29, 2003 (downloaded from [6]) are used to perform data-replay analysis for 9 and 3 independent station pairs, respectively, with separations from 23 to 75 km. These station locations are shown on the maps in Figure 7 with maximum gradient values (see [7]) in mm/km in green and with green lines connecting the pairs of stations from which the estimations were computed. A dashed red line indicates the position and orientation of the ionosphere anomaly shown in Figure 2 at around 2100 UT. The 9

station pairs which were used for data-replay analysis in the OH region are GARF/GUST, WOOS/GARF, FREO/LSBN, COLB/MTVR, ZOB1/GARF, SIDN/KNTN, STKR/MCON, GALB/LEBA, and ERLA/GALB. The 3 station pairs in the NC region, in order of distance between two stations, are FAYR/RALR, LILL/RALR, and SNFD/RALR. In order to get the worst-case vertical position error (VPE), one station, which the ionosphere front hits first, is treated as a static LAAS user, and the other station, which ionosphere front hits later, is treated as a LAAS reference facility.

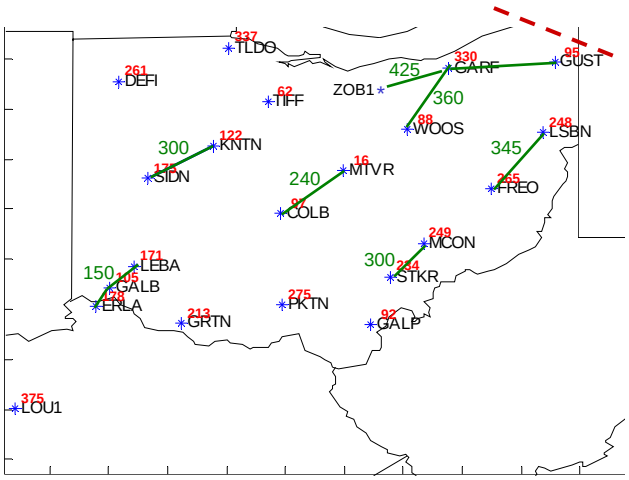

(a)

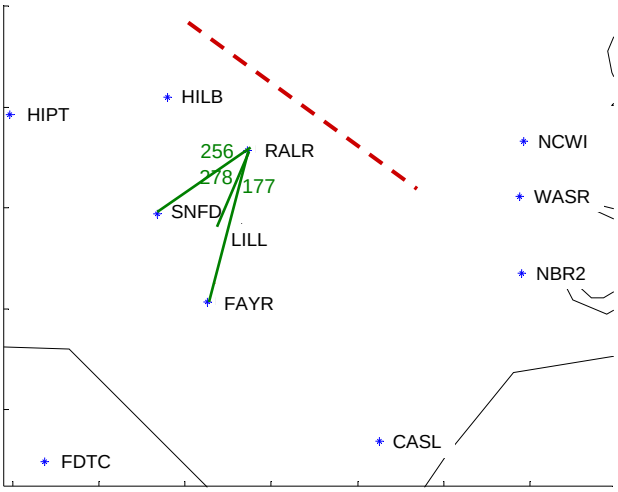

(b)

Figure 7: Map of CORS stations (a) in OH; and (b) in NC, and ionosphere slopes observed and validated with both dual-frequency and L1-only data around 2100 UT. Solid green lines connect pairs of stations, and slope estimates are indicated. The dashed red line marks the approximate orientation and position of the ionosphere filament edge at 2100 UT.

2.3 Methodology

The Data-Replay analysis procedure is based on traditional differential GPS. The detailed procedure for data-replay analysis is shown in Figure 8 and is listed below:

1) Assign the stations within a station pair such that the station impacted first by a severe ionosphere gradient is treated as a stationary LAAS pseudo-user, and the other station is treated as the LGF;
2) Compare LGF pseudorange to the distance from LGF to satellites to compute LGF corrections;
3) Subtract LGF corrections from pseudo-user pseudorange to obtain the corrected pseudorange between the two stations and compute the resulting VPE;
5) Screen the resulting VPE by checking the computed pseudo-user vertical protection level (VPL) and remove any "bad" geometry whose VPL is higher than VAL;
6) Repeat the procedure described above for all possible "subset" geometries that the aircraft theoretically might use from the set of visible and usable satellites by considering all independent one-satellite-out and two-satellites-out cases;
7) Determine the worst-case (maximum) VPE among the VPE of all possible "subset" geometries for each epoch in time.

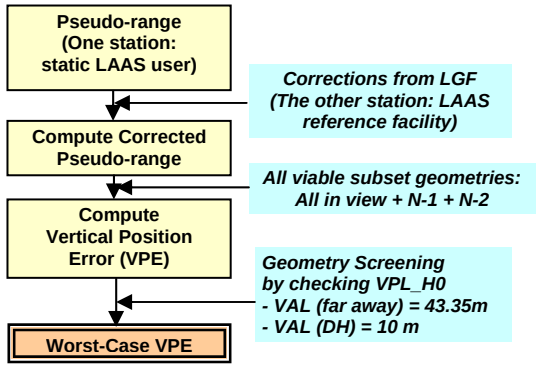

Figure 8: Data-Replay Analysis Procedure

In the simplified geometry screening process used here, two values are used as the vertical alert limit (VAL). One is 43.35 meters, which is the VAL for a large user-to-threshold separation in the LAAS MOPS [8], and the other is 10 meters, which represents VAL at the landing threshold for a minimum decision height of 200 ft. Note that no σ_{pr_gnd}, σ_{vig}, or (ephemeris) P-value inflation is applied in this process to limit geometries beyond what would be allowed by the typical sigmas and P-values that would be broadcast by LAAS absent an ionosphere spatial gradient threat.

3.0 RESULTS

3.1 Ohio Cluster Data-Replay Analysis

In order to help to understand the results of this work, ionosphere delays observed on SVN 38 at 7 CORS stations in the Ohio/Michigan (OH/MI) region are shown in Figure 9 (this was previously reported in [2]). Here, the *x*-axis is GPS time in 10 minute intervals (the traces last about 350 minutes), and the *y*-axis represents slant delay in meters. In this plot, all traces follow each other closely, which indicates that a very similar anomaly front crossed those stations one after another.

As can be seen in Figure 9, the ionosphere delay increased from near zero to about 30 meters in the first 100 minutes as the lines of sight entered the finger-shaped region shown in Figure 2. Then several smaller-scale variations occurred during the period from 100 to 200 minutes. This was followed by an extremely sharp falloff, where the delay dropped about 25 meters in less than 10 minutes as the lines of sight left the finger-shaped region. From 200 minutes onward, the delays increased slowly until SVN 38 set. A gradient of more than 300 mm/km was found during this sharp falling edge at around 2100 UT in previous work [5]. In fact, as shown in Figure 7(a), a gradient of as large as 425 mm/km was observed between CORS stations ZOB1 and GARF at this time (the ionosphere delay observed by ZOB1 is not shown in Figure 9).

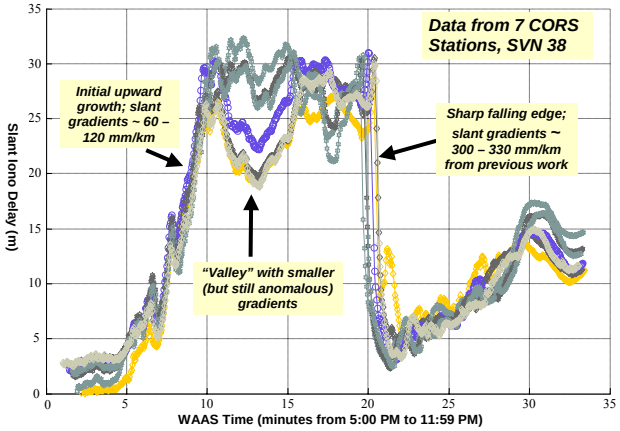

Figure 9: Ionosphere Delay Observed at Seven CORS Stations in OH/MI Cluster in [2]

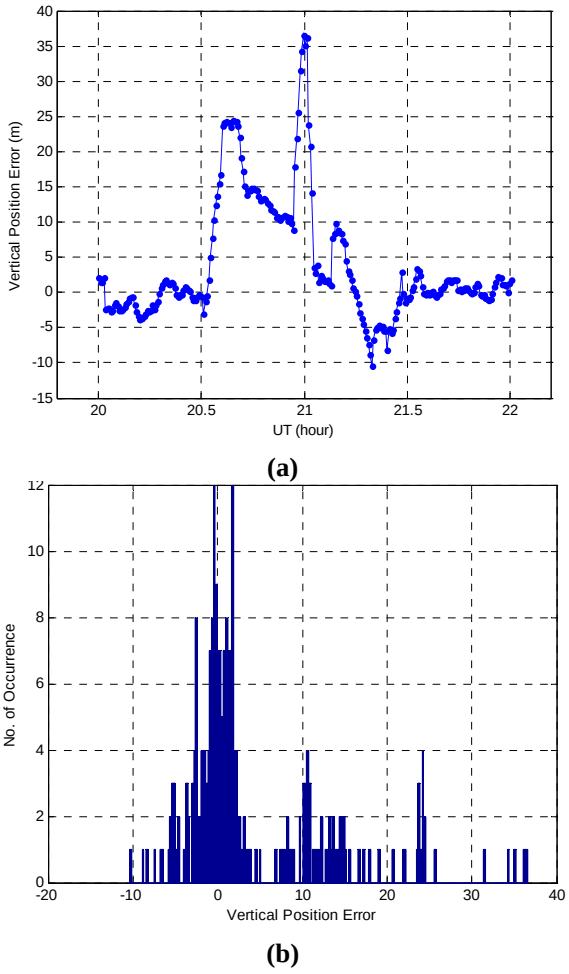

Figure 10: (a) VPE plot; and (b) VPE Histogram for WOOS/GARF

Data-replay analysis of two pairs of stations, WOOS/GARF and ERLA/GALB, in the Ohio region is shown in detail in this paper. First, for the WOOS/GARF pair, GARF is treated as a pseudo-user and WOOS is treated as an LGF since the ionosphere front hit GARF first and then WOOS later, as can be seen in Figure 7(a). The separation of this station pair is 74.5 kilometers, and the maximum gradient value was 360 mm/km as noted in Figure 7(a). Figure 10(a) shows a plot of VPE over time and Figure 10(b) shows a VPE histogram for WOOS/GARF when the pseudo-user (GARF) applies all GPS satellites visible at the time the observations were made (as a function of UT in hours in Figure 10(a)). The peak error corresponds to the sharp falling edge in Figure 9 at around 2100 UT. The maximum error of 37 meters occurs when the maximum gradient occurs, as expected.

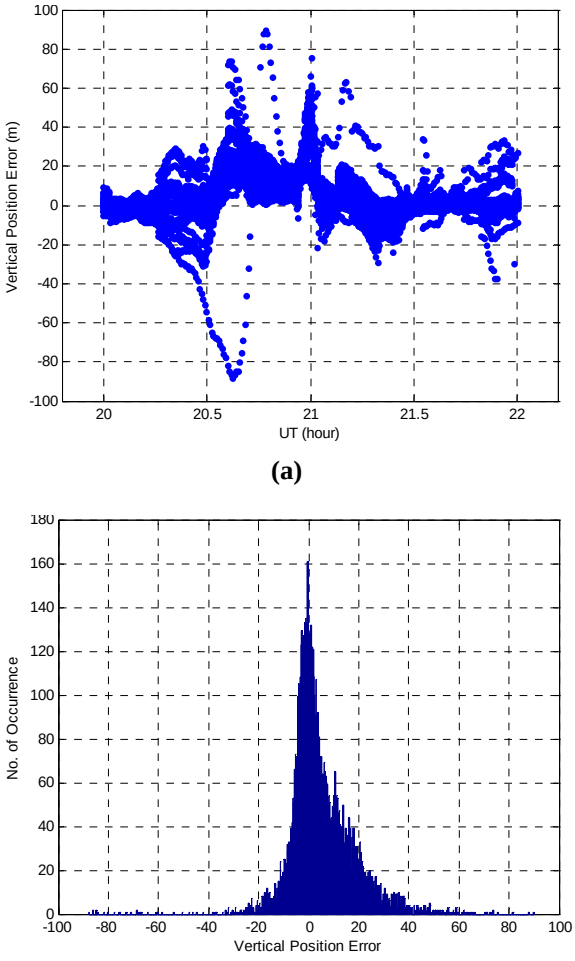

Figure 11: (a) VPE plot; and (b) VPE Histogram of all-in-view + N-1 + N-2 for WOOS/GARF with VAL = 43.35 m

Figure 11 shows the VPE plot and VPE histogram for WOOS/GARF when all possible "subset" geometries from the set of visible and usable satellites are added and a VAL of 43.35 meters is applied for geometry screening. When these subset geometries are included, the maximum error increases from 37 meters to 91meters. The largest error does not correspond to the maximum gradient in Figure 9. Instead, it results from a bad subset geometry which is not screened out by a VAL of 43.35 meters. The fact that one subset of geometry has a large error for a single epoch is seen in Figure 11(a). The VPE of this subset corresponds to the "tail" part of the VPE histogram in Figure 11(b).

Switching to a tighter VAL of 10 meters screens out many more "bad" geometries, and the bad subset geometry remained in Figure 11 is gone, as can be clearly seen in Figure 12(a). The maximum error is down to 62 meters in Figure 12(b). From Figures 11 and 12, it is clear that the worst-case VPE screened by VAL = 10m is no larger than the one screened by VAL = 43.35 m, as expected from theory.

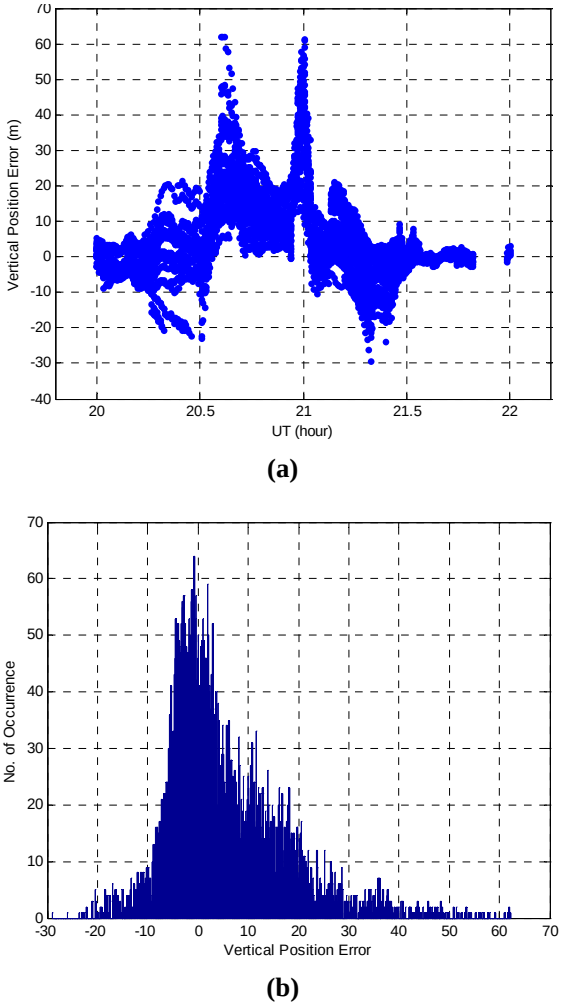

Figure 12: (a) VPE plot; and (b) VPE Histogram of all-in-view + N-1 + N-2 for WOOS/GARF with VAL = 10 m

The second station pair examined in detail here is ERLB/GALB. These two stations are separated by 23.5 kilometers, and the maximum ionosphere gradient at around 2100 UT is 150 mm/km in Figure 7(a). Note that this pair has both a smaller separation and a smaller maximum ionosphere gradient than the WOOS/GARF pair. Also, the time when the ionosphere front hit this pair is after 2100 UT. The VPE plot vs. time and the VPE histogram for ERLB/GALB when all visible satellites are used are plotted in Figure 13. The smaller separation and smaller ionosphere gradient give a maximum error of 9 meters, which is much smaller than the one for WOOS/GARF, and this error occurs after 2100 UT.

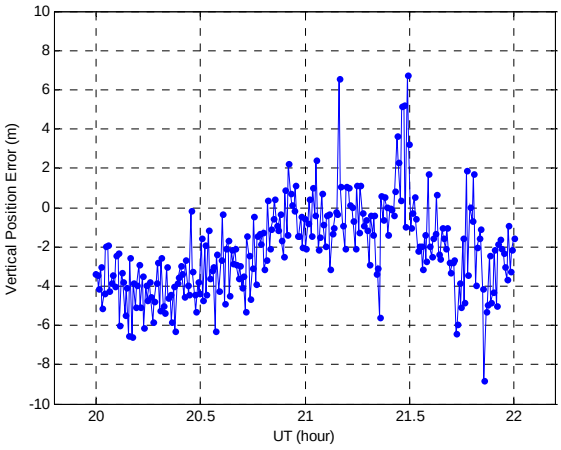

(a)

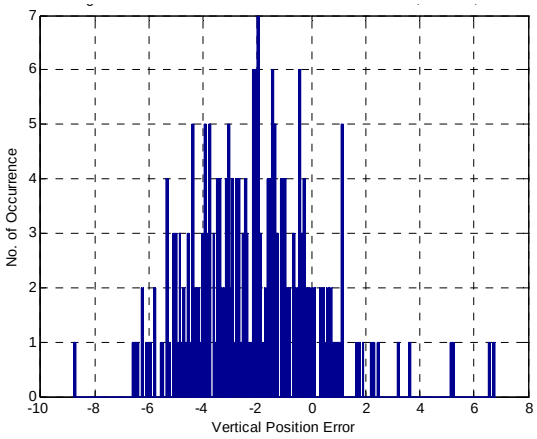

(b)

Figure 13: (a) VPE; and (b) VPE Histogram for ERLA/GALB

The VPE plot and VPE histogram for ERLA/GALB for all possible subset geometries with geometry screening using a VAL of 43.35 meters are shown in Figure 14. Including subset geometries raises the maximum VPE from 9 meters to 40 meters. It occurs early, before the large falloff in ionosphere delay, and there is a big gap between this maximum error and the next-largest error on the histogram in Figure 14(b), which suggest that this result is again driven by a bad geometry and not by the ionosphere gradient. Therefore, it is not likely to pass geometry screening using a VAL of 10 meters. When a VAL of 10 meters is applied, the worst-case VPE drops from 40 meters to 18 meters, as shown in Figure 15. Figure 15 shows the VPE plot and VPE histogram for ERLA/GALB with all possible subset geometries and geometry screening using a VAL of 10 meters.

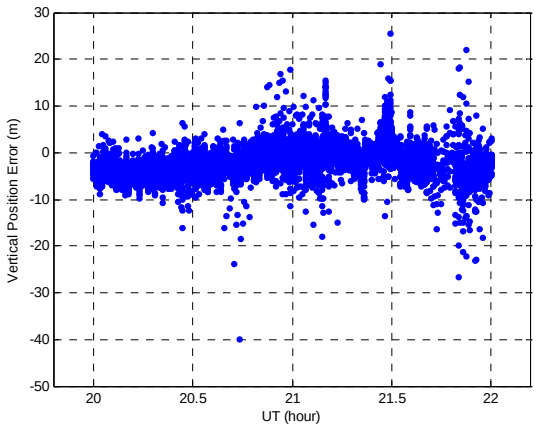

(a)

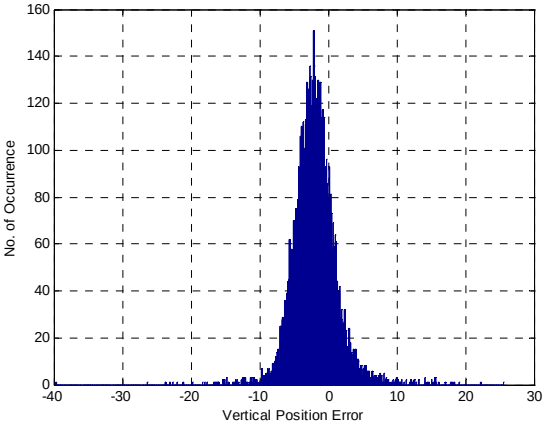

(b)

Figure 14: (a) VPE; and (b) All-in-view + N-1+N-2 of All-in-view + N-1 + N-2 for ERLA/GALB with VAL = 43.35 m

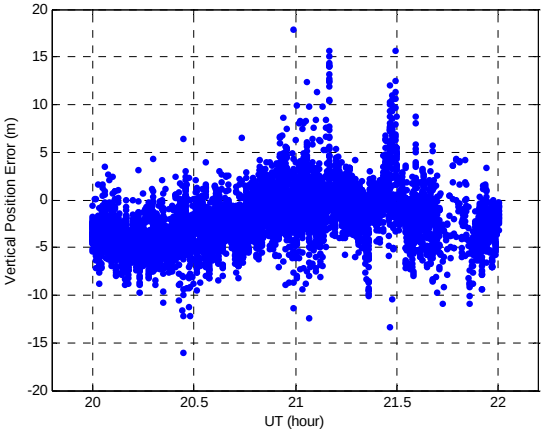

(a)

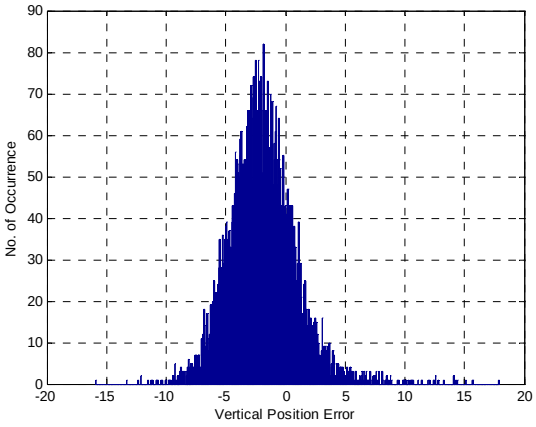

(b)

Figure 15: (a) VPE; and (b) VPE Histogram of all-in-view + N-1 + N-2 for ERLA/GALB with VAL = 10 m

The worst-case VPE as a function of station separation in the Ohio region on November 20, 2003 is summarized in Table 1 and Figure 16. Red stars in Figure 16 and numbers in the third column of Table 1 indicate worst-case VPE values with VAL = 43.35 meters, and the red line in Figure 1 shows a least-square fit to these results. Blue stars in Figure 16 and numbers in the fourth column of Table 1 indicate worst-case VPE values with VAL = 10 meters, and the blue line in Figure 16 shows the least-square fit to these results. From these two fits, it can be confirmed that the worst-case VPE tends to increase as separation increases and that worst-case VPE screened by the looser VAL of 43.35 meters tends to be larger than that screened by the tighter VAL of 10 meters.

Table 1: Summary of Worst-case VPE in OH on November 20, 2003 (in meters)

Station Pair (LGF – USER)	Separation (km)	VAL (m)	
		43.35	10
GARF-GUST	75.3	63.87	52.53
WOOS-GARF	74.5	91.01	62.20
ZOB1-GARF	51.2	80.56	80.56
FREO-LSBN	73.6	92.60	59.78
SIDN-KNTN	59.1	74.62	46.53
COLB-MTVR	65.4	139.81	51.09
STKR-MCON	44.2	86.01	53.17
GALB-LEBA	29.8	32.92	28.13
ERLA-GALB	23.5	39.73	17.90

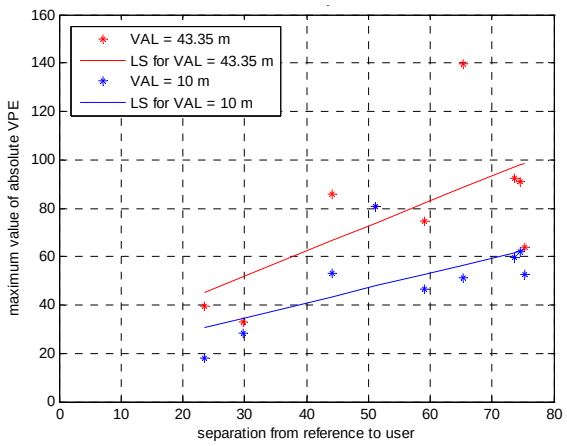

Figure 16: Worst-case VPE as a Function of CORS Station Separation

3.2 North Carolina Cluster Data-Replay Analysis

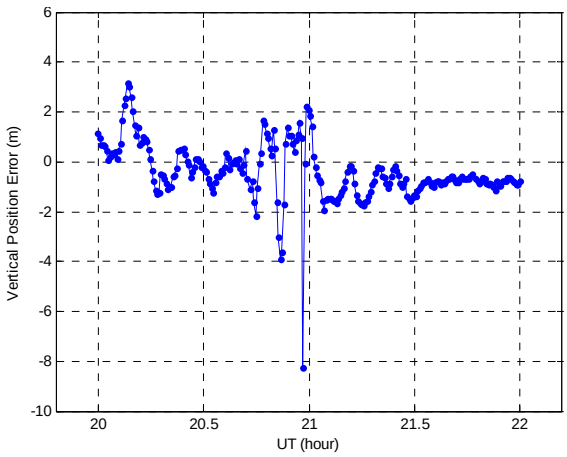

(a)

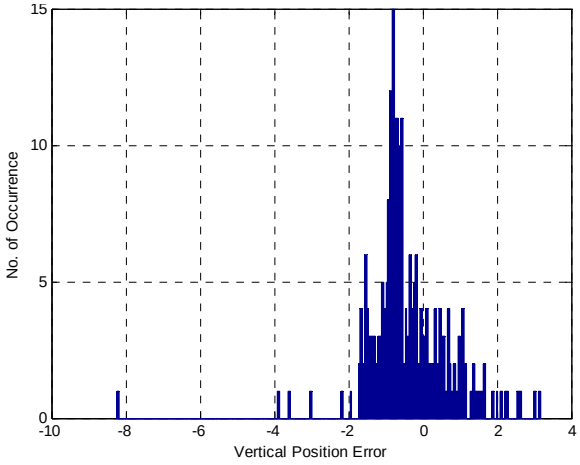

(b)

Figure 17: (a) VPE; and (b) VPE Histogram for LILL/RALR

To demonstrate data-replay analysis in the NC region on October 29, 2003, the LILL/RALR pair is chosen since it has the smallest separation of 45.9 kilometers and the largest maximum gradient of 278 mm/km among the three station pairs which have been examined in this region, as shown in Figure 7(b). The VPE plot and VPE histogram for LILL/RALR for the all-in-view geometry are plotted in Figure 17. The very sharp peak in Figure 17(a) occurs because ionosphere front moved very quickly in this region at the time the observations were made. That is why the maximum VPE is 8 meters, which is very small when a separation of 45.9 km and a relatively higher ionosphere gradient are considered. The fast-moving ionosphere front is also a reason why the maximum VPE of 8 meters is far away from most values in the histogram, which are smaller than 4 meters.

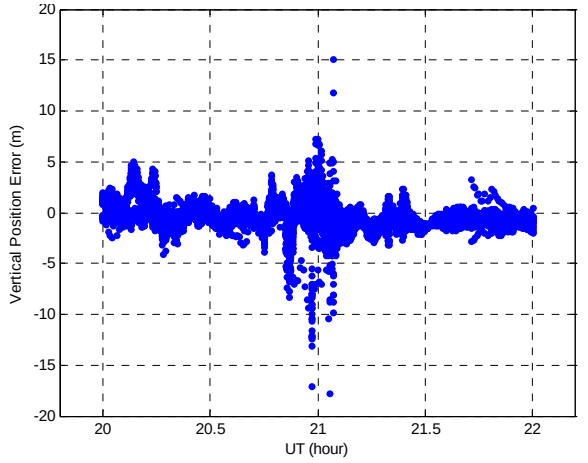

(a)

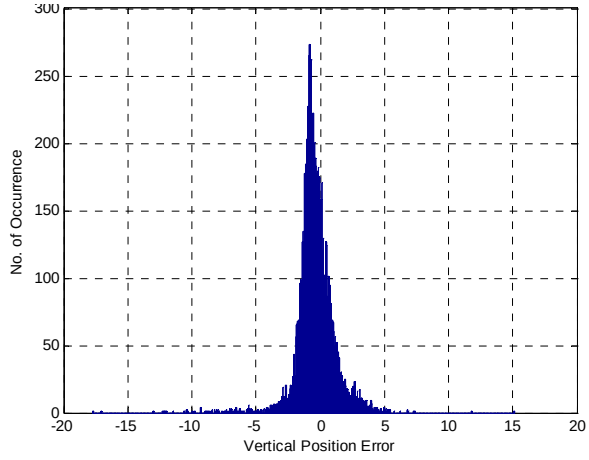

(b)

Figure 18: (a) VPE and (b) VPE Histogram of all-in-view + N-1 + N-2 for LILL/RALR with VAL = 43.35.

Figure 18 shows the VPE plot and VPE histogram for LILL/RALR including all possible subset geometries obtained by taking all independent one-satellite-out and two-satellites-out combinations among the visible satellites. Geometry screening is performed using a VAL of 43.35 meters. Adding worse subset geometries pushes the maximum error from 8 meters to 18 meters. As can be seen in Figure 18(a), the VPE corresponding to the maximum gradient is near the worst-case VPE.

Geometry screening by checking if VPL is less than a VAL of 10 meters (see Figure 19(a)) gets rid of some points from Figure 18(a), but the worst-case VPE in Figure 18 survives this tighter geometry screening. Thus, the maximum VPE is the same as that with a VAL of 43.35 meters.

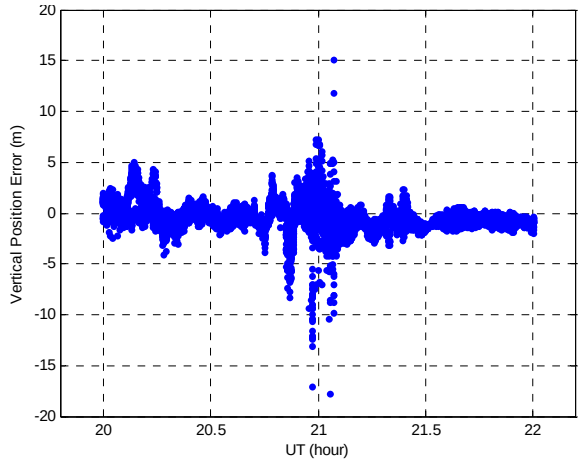

(a)

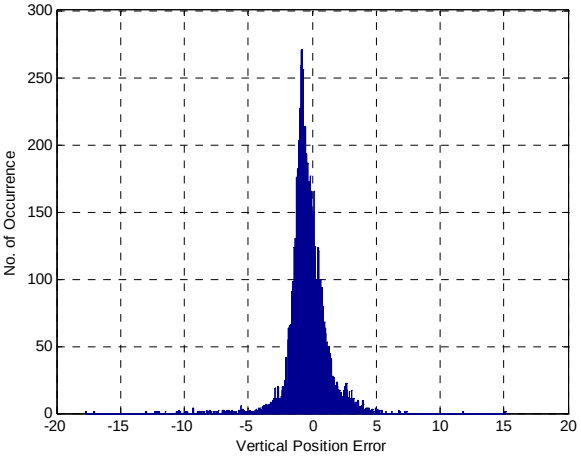

(b)

Figure 19: (a) VPE; and (b) VPE Histogram of all-in-view + N-1 + N-2 for LILL/RALR with VAL = 10 m.

The worst-case VPE as a function of separation on October 29, 2003 in the NC region is summarized in Table 2. The third column of Table 2 indicates the worst-case VPE with a VAL = 43.35 meters, and the fourth column of Table 2 indicates the worst-case VPE with VAL = 10 meters. Note that, while tighter geometry

screening (using a 10-meter VAL) does not affect the maximum VPE for the LILL/RALR station pair, it does reduce the maximum VPL for the other two station pairs listed (FAYR/RALR and SNFD/RALD).

Table 2: Summary of Worst-case VPE in NC on October 29, 2003 (in meters)

Station Pair (LGF – USER)	Separation (km)	VAL (m)	
		43.35	10
FAYR-RALR	86.1	22.66	15.90
SNFD-RALR	58.5	14.72	13.48
LILL-RALR	45.9	17.70	17.70

4.0 CONCLUSIONS

The objective of this work is to complement the results of worst-case ionosphere anomaly simulations and provide a potentially more-realistic depiction of the impact of specific validated ionosphere anomalies on LAAS users. Data-replay analysis provides a different viewpoint on LAAS vulnerability that do the worst-case ionosphere simulations detailed in [1] because it is limited to events that actually occurred as opposed to worst-case extrapolations of threat-model parameters gleaned from observed events.

In this study, several comparisons of the results of data-replay analysis with the result of worst-case simulation were made. First, despite having very large separations between CORS stations compared to typical LGF-to-user separations in LAAS and the lack of a moving user, worst-case VPE and VPE histograms are similar (to first order) to those given by simulation methods. Second, the roughly linear increase of VPE with separation is as expected (a similar growth patter results from simulation). Third, the reduction in worst case VPE when VAL is reduced to 10 meters is similar to the impact of geometry screening when implemented in simulation. These results, while not supporting exact one-to-one comparisons with simulation, support the notion that the worst-case ionosphere simulations used in LAAS CAT I ionosphere mitigation analysis and parameter inflation calculations are at least reasonable and are probably conservative.

ACKNOWLEDGMENTS

The constructive comments and advice regarding this work provided by many other people in the Stanford GPS research group pare greatly appreciated. This study was supported by the Federal Aviation Administration (FAA) Local Area Augmentation System (LAAS) Program Office. Within the FAA, Carlos Rodriguez, John Warburton, and Barbara Clark were particularly helpful. The opinions discussed here are those of the authors and do not necessarily represent those of the FAA or other affiliated agencies.

REFERENCES

[1] J. Lee, M. Luo, S. Pullen, Y.S. Park M. Brenner, and P. Enge, "Position-Domain Geometry Screening to Maximize LAAS Availability in the Presence of Ionosphere Anomalies," *Proceedings of ION GNSS 2006*, Fort Worth, TX, September 26-29 , 2006, pp. 393-408.

[2] M. Luo, S. Pullen, s. Datta-Barua, G. Zhang, T. Walter, and and P. Enge, "LAAS Study of Slow-Moving Ionosphere Anomalies and Their Potential Impacts," *Proceedings of ION GNSS 2005*, Long Beach, CA, September 13-16, 2005, pp. 2337-2349.

[3] M. Luo, "End-around-Check with LGF Monitor," Stanford University, Unpublished Presentation, May 3, 2005.

[4] A. Ene, D. Qiu, M. Luo, S. Pullen, and P. Enge, "A Comprehensive Ionosphere Storm Data Analysis Method to Support LAAS Threat Model Development," *Proceedings of ION 2005 National Technical Meeting*, San Diego, CA., January 15-20, 2005, pp. 110-130.

[5] M. Luo, s. Pullen, A. Ene, D. Qiu, T. Walter, and P. enge, "Ionosphere Threat to LAAS: Updated Model, User Impact, and Mitigations," *Proceedings of ION GNSS 2004*, Long Beach, CA., September 21-24, 2004, pp. 2771-2785.

[6] National Geodetic Survey (NGS) – CORS Data and Related Information. URL: http://www.ngs.noaa.gov/CORS/download2.

[7] G. Zhang, J. Lee, S. Datta-Barua, S. Pullen, and P. Enge, "Low-Elevation Ionosphere Spatial Anomalies Discovered from the 20 November 2003 Storm," *Proceedings of ION 2007 National Technical Meeting*, San Diego, CA., January 22-24, 2007, http://waas.stanford.edu/~wwu/papers/gps/PDF/ZhangIONNTM07.pdf.

[8] *Minimum Operational Performance Standards for GPS Local Area Augmentation System Airborne Equipment.* RTCA, Washington, D.C., RTCA SC-159, WG-4A, DO-253A, November 28, 2001.

[9] M. Luo, S. Pullen, J. Dennis, H. Konno, G. Xie, T. Walter, S. Datta-Barua, T. Dehel, and Per Enge "LAAS Ionosphere Spatial Gradient Threat Model and Impact of LGF and Airborne Monitoring," *Proceedings of ION GPS*

2003, Portland, OR., September 9-12, 2003, pp 2255-2274.

[10] M. Luo, S. Pullen, T. Walter, and P. Enge, "Ionosphere Spatial Gradient Threat for LAAS: Mitigation and Tolerable Threat Space", *Proceedings of ION 2004 Annual Meeting*, San Diego, CA., January 26-28, 2004.